Stress Relaxation of Star/Linear Polymer Blends

Jung Hun Lee and Lynden A. Archer*

School of Chemical Engineering, Cornell University, Ithaca, New York 14853

Received March 15, 2002; Revised Manuscript Received June 7, 2002

ABSTRACT: Stress relaxation dynamics in a series of star/linear 1,4-polybutadiene blends with fixed star-arm molecular weight M_a, variable linear polymer molecular weight M_L, and variable star polymer volume fraction ϕ_s are investigated. Storage and loss moduli, $G'(\omega)$ and $G''(\omega)$, obtained from small amplitude oscillatory shear experiments are compared with predictions of a parameter-free molecular theory for star/linear blend dynamics. For star/linear blends with moderate star polymer concentrations $\phi_s \approx 0.28$, theoretical $G'(\omega)$ and $G''(\omega)$ are found to be in good to excellent accord with experimental results over the entire range of frequencies and M_L values studied. The quality of the predictions worsen as star polymer concentration is varied in either direction (i.e., higher or lower). At low ϕ_s, the greatest discrepancies between theory and experiment are observed at oscillation frequencies $\omega \leq \omega_d$, where $\omega_d^{-1} \sim M_L^{3.4\pm0.25}$ is approximately the terminal time of linear polymer molecules in the blends. A theoretical analysis based on the idea that constraint release progresses by Rouse motion in a narrow *exploring tube* confined in a larger *super tube* yields a theory with better predictive properties for blends with low star polymer concentration. A new criterion is proposed for determining whether relaxation in star/linear polymer blends goes to completion after constraint release.

Introduction

Blends of chemically similar starlike and linear polymer molecules (star/linear blends) provide simple model systems for studying relaxation dynamics in branched polymer liquids. Experimental studies of star/linear blend viscoelasticity are important because they provide a direct means of evaluating molecular theories for branched polymer dynamics.[1,2] All dynamic regimes manifested by complex branched polymer topologies can, for instance, be accessed in star/linear blends by appropriate selection of star-arm molecular weight $M_a = m_0N_a$, linear polymer molecular weight $M_L = m_0N_L$, and volume fraction of star polymer ϕ_s. Most commercial long-chain branched polymers contain significant amounts of unbranched materials by design (to produce materials with more balanced rheological properties that improve processability) or by accident (heterogeneities in catalyst structure and activity yield polymers with heterogeneous architectures). Star/linear blends can serve as model materials in this situation because the effect of linear polymer fractions on overall relaxation dynamics of branched molecules can be isolated.

The number of experimental studies of relaxation dynamics in model star/linear polymer blend systems is surprisingly small.[3−6] These studies nonetheless provide dramatic evidence of the rich variety and complexity of dynamic processes that can be introduced into a branched polymer by blending it with linear molecules. At low star polymer volume fractions, terminal dynamics have been found, for example, to be dominated by constraint release processes.[3,4,6] However, even in these materials, terminal properties (zero-shear viscosity η_0 and longest relaxation time τ_{d0}) depend more weakly on linear polymer molecular weight than expected from all[7−9] but two theories of constraint release in polymer blends.[10,11] At higher ϕ_s, relaxation dynamics in star/linear blends become more complicated, and terminal properties depend on ϕ_s and M_L in ways that are not entirely understood.[5,6]

Recently, Milner and co-workers[1] proposed a framework for studying relaxation dynamics in star/linear homopolymer blends. This model will be referred throughout the article as the MM model. The MM model's two main features are that it assumes relaxation dynamics in star/linear blends are hierarchical and that relaxed outer segments of a star-arm can degrade the entanglement structure in which inner-arm segments relax (dynamic dilution).[12] Thus, at early times following imposition of a small deformation, relaxation of the outermost segments of linear and star molecules proceeds by activated retraction processes.[13]

At longer times, linear polymer relaxation by reptation diffusion outcompetes activated relaxation for relieving stress. In star polymers comprised of equal-sized arms, reptation diffusion is suppressed on any time scale by the branch point. The activated retraction process therefore continues until arm segments completely diffuse out of their primitive tubes. The retraction process is nonetheless different from that of a pure star polymer because reptational diffusion of linear molecules degrade the entanglement structure in which star arms relax. Even though the opposite situation can also be imagined (i.e., retraction of outer star-arm segments altering the tube structure in which long linear polymer molecules reptate), this requires that arm retraction of the affected linear segments be competitive with reptation; i.e., the process is only important at early times. Thus, the overall long-time response can be captured by activated relaxation of star arms in a dynamically diluted network environment and by reptation of linear molecules in a fixed network.

The most challenging questions about dynamics in star/linear polymer blends arise from the fact that linear polymer reptation and star-arm retraction occur on very different time scales for realistic N_a/N_e and N_L/N_e values. Thus, as the linear polymer chains reptate, they degrade the entanglement environment in which star arms relax. A related challenge arises when the linear polymers have completely vacated their original tubes.

10.1021/ma020398e CCC: $22.00
Published on Web 07/16/2002

In this case, two situations can be imagined. In the first, disappearance of the linear polymer constraints so perforate the entanglement structure that the effective tube diameter $a_e(\tau_{dL})$ becomes comparable to or larger than the coil size R_a^* of unrelaxed arm segments. In this situation, Rouse relaxation is the most plausible mechanism by which unrelaxed star-arm segments unload their remaining stress. On the other hand, if $R_a^* \gg a_e(\tau_{dL})$, arm segments remain well entangled even after the linear molecules have relaxed. In this case, the final relaxation would be expected to proceed as before τ_{dL}, i.e., by arm retraction in a dilated tube.

This simple picture of relaxation dynamics in star/linear polymer blends may not hold in practice for a variety of reasons. First, relaxed outer arm segments may not be as effective network diluents for inner segments near the branch point of a star molecule. Second, relaxed linear chains may exert an influence on star-arm dynamics that is qualitatively different from that of a low molecular weight solvent. Specifically, when a linear molecule releases an entanglement with a section of a star arm, the section is only allowed a finite time $O(\tau_e)$ to lose orientation before the entanglement is reestablished by another molecule. The limitations this pose on constraint release relaxation of star arms is anticipated to be particularly severe for arm segments near the branch point, which might relax virtually as if the constraint is not lost. Finally, there may be other modes of relaxation possible in star/linear blend systems that have not yet been accounted for in tube-model theories. For example, a recent analysis of relaxation dynamics of star/linear polymer blends, based on Bueche's drag coupling model,[14] yielded the following expression for the relaxation time of star arms

$$\tau_{d,a} \sim \frac{\tau_e}{s}\left[\left(\frac{N_a}{N_e}\right)^2 + \frac{\phi_L}{\phi_a}\frac{N_a N_L}{N_e^2} + \frac{s}{2}\frac{\phi_L}{\phi_a}\frac{N_a N_L^2}{N_e^3}\right] \times \left(\exp\left[s\phi_s\frac{N_a}{N_e}\right] - 1\right)$$

where s is a *coupling parameter* ($0 \le s \le 1$) that reflects the strength of secondary bonds between molecules in the blend.[6] The same approach used to derive this equation yields expressions for the relaxation time in pure star and linear polymers that are virtually identical to those provided by early tube model theories that did not account for the effects of contour length fluctuations, constraint release,[15] and dynamic dilution.[13] Some of the scaling forms in the drag-coupling model expression for $\tau_{d,a}$ are also recognizable in terms of known tube-model physics, but many are not. Experimental studies of relaxation dynamics in star/linear blend systems should help determine which, if any, of these new modes of relaxation are important.

Experiment

Linear (L) and six-arm star (S) 1,4-polybutadiene (PBD) samples used in this study were purchased from Polymer Source Inc.. Molecular weights and polydispersity indices of all polymers used in the study (see Table 1) were characterized using a size exclusion chromatograph equipped with a multi-angle laser light scattering detector. A single six-arm star polymer with equal arm molecular weights $M_a = 73\,000$ was used for the entire study. Star/linear 1,4-polybutadiene blends were prepared by dissolving desired amounts of linear and star PBD in excess dichloro methane (methylene chloride, Aldrich). The methylene chloride was subsequently allowed to evaporate at room temperature for a few weeks to produce the final star/linear melt blend with the desired composition. Sample names referenced in the table are coded by molecular weight and volume fraction ϕ_s of star polymer in the blends. For example, L129K refers to a linear polymer with $\bar{M}_n = 129\,300$, while a sample coded SL129K10 is a star/linear polymer blend containing L129K and 10 vol % of the six-arm star.

Table 1. Molecular Weight of Linear Polybutadiene Melts

linear sample	M_n	PDI[a]
L18K	18 000	1.03
L48K	48 000	1.04
L67K	67 300	1.04
L87K	87 000	1.05
L129K	129 300	1.03
L176K	176 400	1.03
L246K	246 200	1.04
L336K	336 000	1.07

[a] PDI: polydispersity index.

Dynamic storage $G'(\omega)$ and loss $G''(\omega)$ moduli of the star/linear PBD blend samples were measured in small-amplitude oscillatory shear flow using a Paar Physica Modular Compact rheometer (MCR 300) and a Rheometrics ARES-LS rheometer. Here, 15 mm diameter, stainless steel cone-and-plate fixtures (cone angle, 2.5°) and 10 mm diameter parallel-plate fixtures were used for all experiments reported in the article. In a small number of cases (blends with large ϕ_s), storage and loss moduli information from oscillatory shear experiments were supplemented by data from small-amplitude step strain measurements. $G'(\omega)$ and $G''(\omega)$ were obtained from step shear data by first fitting the measured relaxation modulus $G(t)$ by a sum of exponential functions then determining the respective Fourier sine and cosine transforms of the fitted function. All experiments were performed at 28 °C under a blanket of high-purity nitrogen gas. This approach removes errors that can arise from uncertain validity of time−temperature superposition in branched/linear polymer blend systems and from the possibility of cross-link formation in 1,4-polybutadiene melts at elevated temperature.

Results and Discussion

Dynamic storage, $G'(\omega)$, and loss moduli, $G''(\omega)$, for star/linear polymer blends covering a wide range of star polymer volume fractions and linear polymer molecular weight are provided in Figures 1−4. Figure 1, for example, illustrates the effect of ϕ_s on $G'(\omega)$ and $G''(\omega)$ for star/linear blends with a fixed high molecular weight linear polymer L129K. The results show that while high frequency (short-time) relaxation dynamics are only marginally affected by star polymer volume fraction, long time dynamics are profoundly influenced, particularly at $\phi_s > 0.05$. It is also evident from Figure 1 that low-frequency $G'(\omega)$ and $G''(\omega)$ at different star polymer volume fractions are qualitatively different in distinct ranges of star polymer concentration. The terminal relaxation time $\tau_{d0} = \eta_0 J_e^0$ of L129K is approximately 0.2 s. So, in the absence of substantial slowing down of linear polymer relaxation by the star arms, the largest effect of ϕ_s is evident when the linear chain contribution to blend rheology is likely minimal. Qualitative differences between $G'(\omega)$ and $G''(\omega)$ measured at different ϕ_s can therefore be understood by making use of the idealization of extremely long star arms diffusing in a rapidly reptating linear polymer network. Specifically, if relaxed linear molecules are assumed to function as effective solvents for unrelaxed star arms, the arm entanglement density $(N_a/N_e(\phi_s)) = (N_a\phi_s^{4/3}/N_e)$ following linear polymer relaxation varies from <1 for the 2%

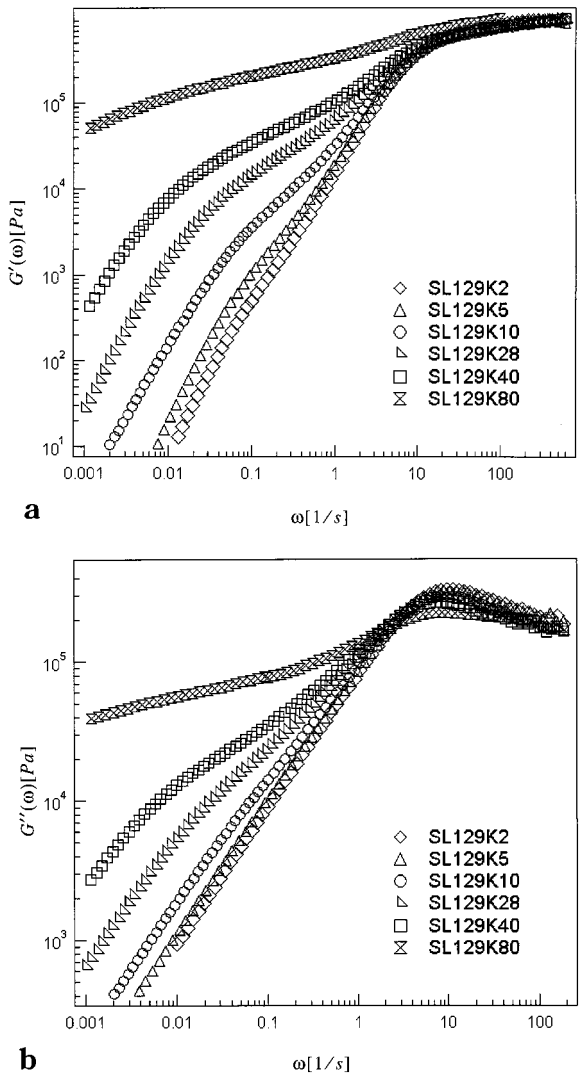

Figure 1. Dynamic moduli, (a) $G'(\omega)$ and (b) $G''(\omega)$, for the SL129KX series star/linear polymer blends with star volume fractions $\phi_s = 0.02$, 0.05, 0.1, 0.28, 0.4, and 0.8.

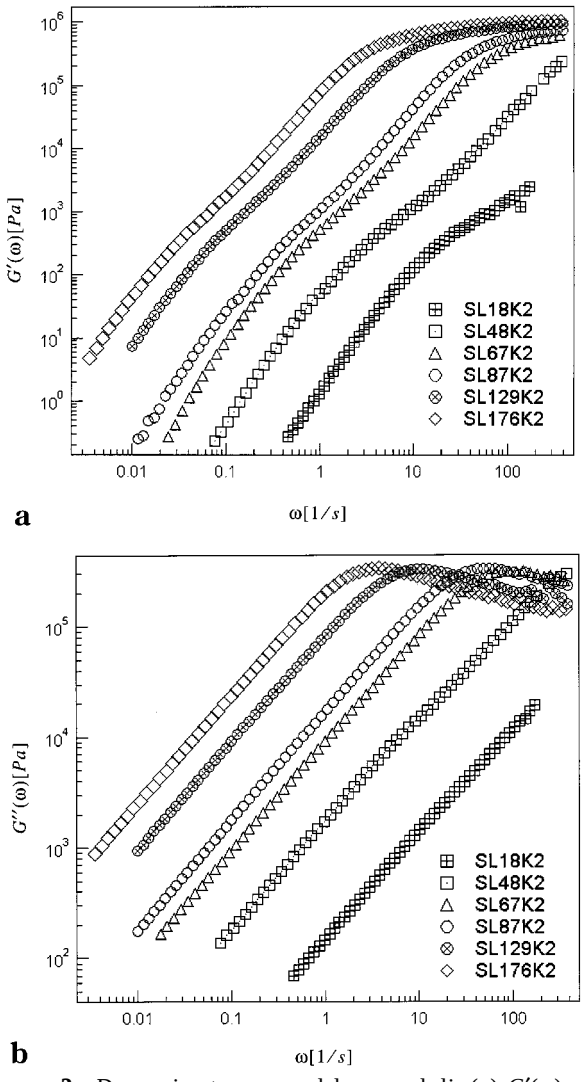

Figure 2. Dynamic storage and loss moduli, (a) $G'(\omega)$ and (b) $G''(\omega)$, of star/linear blends with variable linear polymer molecular weight and fixed star polymer concentration $\phi_s = 0.02$.

blend, to 7 for the 28% material, and eventually to 28 for the 80% star/linear polymer blend. Here we have used $M_e = 1900$. Thus, terminal dynamics spanning the entire range from arm retraction to Rouse diffusion by unentangled arms are anticipated in the systems studied.

Figures 2−4 illustrates the effect of linear polymer molecular weight on relaxation dynamics in star/linear blends with a majority of linear chains. Again, if the faster-relaxing linear polymer component is assumed to act as an effective solvent for the star polymer at long times, the entanglement density of star arms in the 2% and 5% blends are below 1, while $N_a/N_e(\phi_s) \approx 1$ for the 10% blend. Terminal dynamics in these blends should therefore be rather similar, which is indeed what is observed. In fact, these dynamics would be anticipated to be well described by simple Rouse motion of star arms following linear polymer relaxation. Star/linear polymer blends with $\phi_s \leq 0.1$ should therefore provide good model systems for studying dynamics in materials with simultaneously relaxing branched and linear polymer fractions.

We now turn to more quantitative comparisons of the experimental results with theory. As already discussed, the MM model provides a promising framework in which star/linear blend dynamics can be studied. The following parameters will be used throughout the article to compare experimental results with predictions from theory, $G_N = 1.25 \times 10^6$ Pa, $M_e = 1900$, and $\tau_e = 2.4 \times 10^{-7}$ s. While the values for τ_e and M_e are similar to those estimated from oscillatory shear data using linear polybutadienes with similar microstructures to the polymers studied here, the G_N value is slightly larger than the average plateau modulus reported for linear 1,4-polybutadienes.[16] The only additional parameter in the MM model is the dilution exponent α. While the MM model assumes $\alpha = 1$ for simplicity, recent work on multiarm polymer dynamics[17] indicate that α is in fact much closer to the generally accepted value of $^4/_3$.[18] In star/linear polymer blends with low star concentration, dilution would be anticipated to have a strong influence on dynamics, so the choice of α is obviously important. To examine the influence of α, the MM model was reformulated without specifying α. Changes to the set of equations provided in ref 1 for describing relaxation dynamics in star/linear blends are summarized in the Appendix. As expected, for the special case $\alpha = 1$, the MM equations are recovered.

We begin by comparing dynamic moduli for SL129K with high star concentrations ($\phi_s \geq 0.28$) with the model

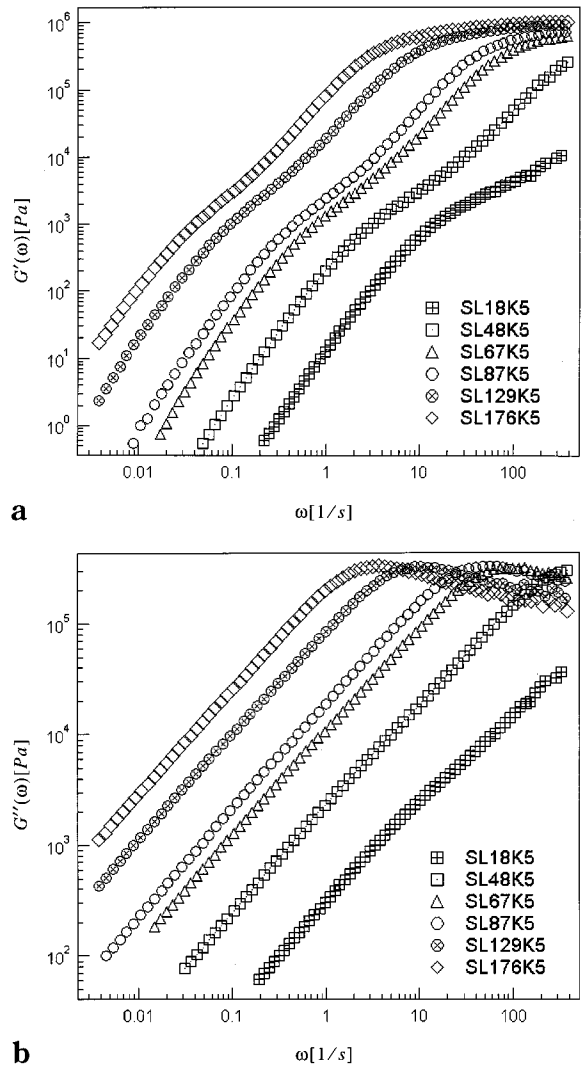

Figure 3. Dynamic storage and loss moduli, (a) $G'(\omega)$ and (b) $G''(\omega)$, of star/linear blends with variable linear polymer molecular weight and fixed star polymer concentration $\phi_s = 0.05$.

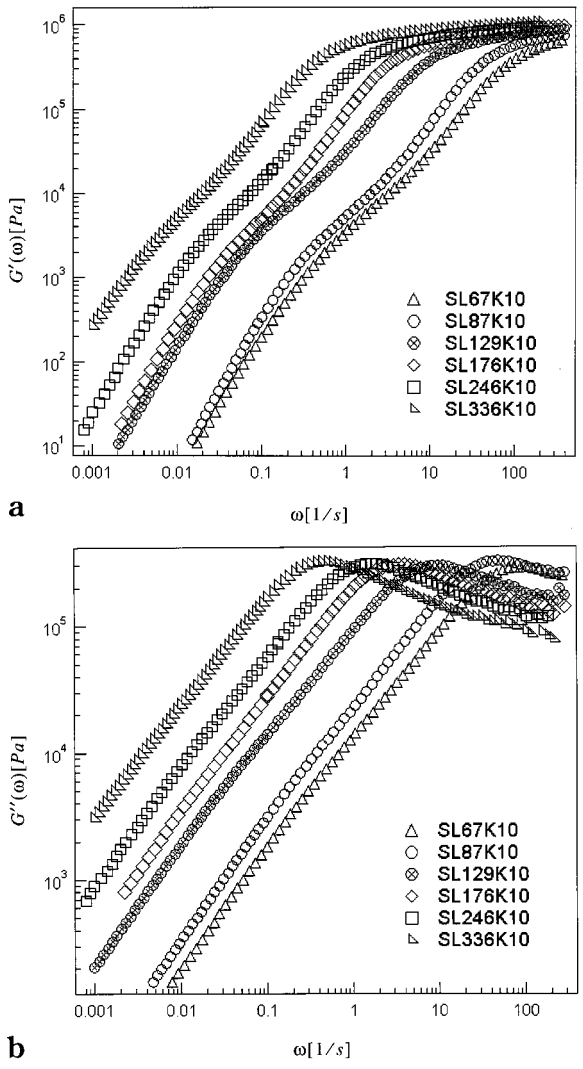

Figure 4. Dynamic storage and loss moduli, (a) $G'(\omega)$ and (b) $G''(\omega)$, of star/linear blends with variable linear polymer molecular weight and fixed star polymer concentration $\phi_s = 0.1$.

predictions. Figure 5 summarizes our observations. The predictions with $\alpha = 4/3$ and 1 are clearly very different. For example, the predicted $G''(\omega)$ and $G'(\omega)$ of SL129K28 with $\alpha = 1$ are similar to the prediction obtained using SL129K40 with $\alpha = 4/3$. The predictions with $\alpha = 4/3$ are also observed to be much closer to the overall experimental data than with $\alpha = 1$. In the case of SL129K28, the predictions with $\alpha = 4/3$ are in excellent accord with the experimental results over the entire frequency range, suggesting that the physical processes governing dynamics in this material are captured well by the theory. As the star concentration is increased, however, the predictions are seen to deviate from the experimental results. The discrepancies between predicted and measured dynamic moduli are initially largest at low oscillation frequencies, but are eventually observed over the full frequency range.

Figure 6 shows the equivalent comparisons for three representative blends, SL129K2, SL176K5, and SL67K10, all with low star polymer concentration ($\phi_s \leq 0.1$). The same model parameters used for the high concentration blends are used here. In this case, the $G''(\omega)$ predictions are seen to be less sensitive to α, and discrepancies between theory and experiment are again most pronounced at low frequency. For example, the largest deviations begin around $\omega = 0.01$ for SL176K5 and $\omega = 1$ for SL67K10, respectively. This should be contrasted with the predictions for $G'(\omega)$, which display much greater sensitivity to α and larger deviations, over a wider frequency range. More careful scrutiny of the plots indicate that the largest deviations between theory and experiment begin just before the "knee" in the low-frequency $G'(\omega)$ curves. The location of the knee is also seen to shift to lower frequencies as M_L is increased, $\omega_d^{-1} \sim M_L^{3.4\pm0.25}$, and is also virtually independent of ϕ_s. Here ω_d is the frequency at the point near the knee (i.e., at which $d(\log[G'(\omega)])/d(\log[\omega])|_{min}$). The knee therefore seems to be associated with the final relaxation of linear chains in the blends.

That the theory incorrectly describes stress relaxation dynamics in the last stages of relaxation can originate from a relatively small number of sources. It is, for example, possible that the unrelaxed arm segments (i.e., following relaxation of the linear chains) are so close to the branch point that the conditions for recovery of dynamic dilution (RDD) are not satisfied. According to the MM model, the criterion for dynamic dilution to be recovered after linear chains relax is $(15/8\alpha)(N_a/N_e)\phi_s^{\alpha}$

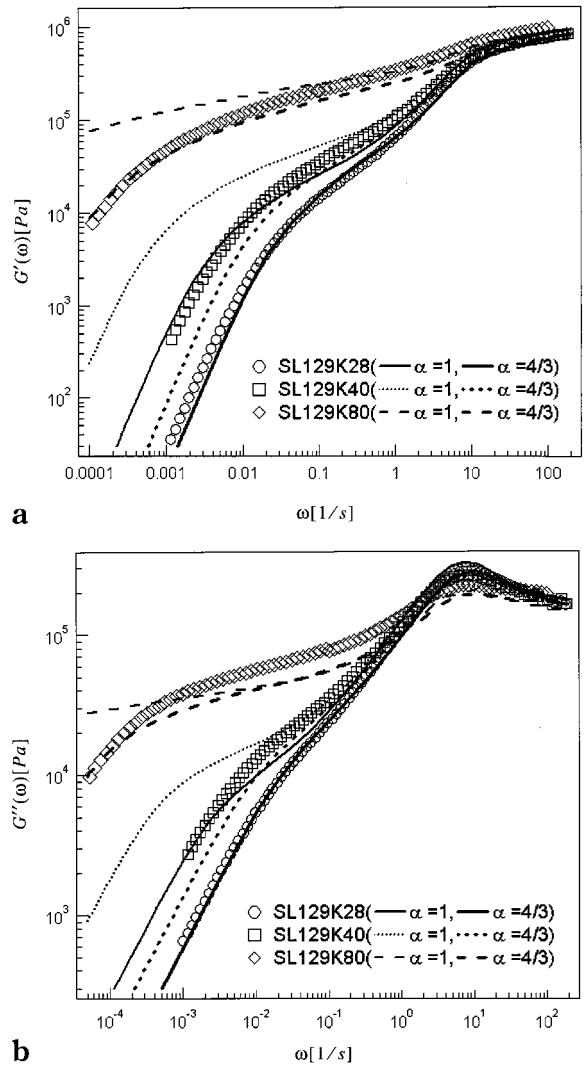

Figure 5. Comparisons of experimental and theoretical storage and loss moduli, (a) $G'(\omega)$ and (b) $G''(\omega)$, for SL129KX star/linear polymer blends. Theoretical predictions are provided using the star/linear blend model of Milner et al.[1] with $\alpha = 1$ (thin line) and $\alpha = 4/3$ (thick line). Parameters used for these comparisons are provided in the text.

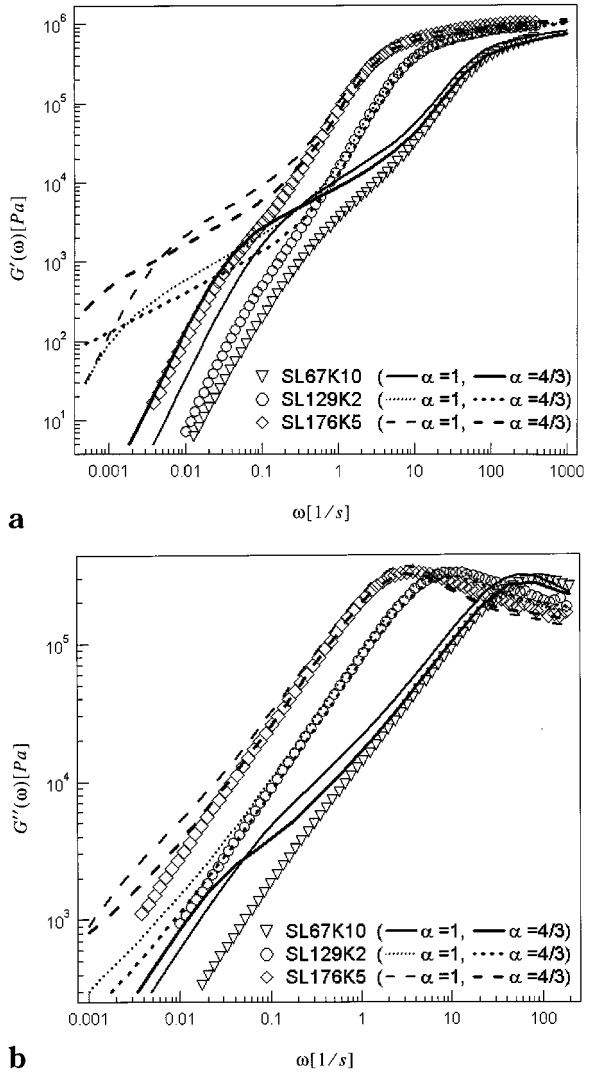

Figure 6. Comparisons of experimental storage and loss moduli, (a) $G'(\omega)$ and (b) $G''(\omega)$, for SL67K10, SL129K2, and SL176K5 with predictions of the MM model, $\alpha = 1$ (thin line) and $\alpha = 4/3$ (thick line).

$s_d[1 - s_d]^{\alpha+1} > 1$. Here, s_d is the fractional distance from the end of a star arm at which the first unrelaxed arm entanglement segment can be located at τ_d, the relaxation time of linear molecules. While this criterion is satisfied by the higher concentration blends in Figure 5, it is violated by all blends in Figure 6. To evaluate the effect of failure of RDD, we simply remove the RDD contribution from the model, by excluding the last term in (A15), and compare the $G'(\omega)$ and $G''(\omega)$ predictions with experiment. The results are shown in Figure 7, parts a and b. It is apparent, particularly from the $G'(\omega)$ results, that even without RDD the model overpredicts both moduli at low frequencies, indicating that RDD cannot be the only source of the discrepancies observed.

A second possibility is that the CR relaxation process terminates faster than assumed by theory. To study this effect, we first review the physics governing arm dynamics following disappearance of entanglements with linear molecules. Immediately following relaxation of linear molecules, star arms are expected to continue relaxing as if they are confined in the same tube as prior to linear polymer relaxation. The arms sense the larger tube created by relaxation of linear molecules only through Rouse-like liberations of their original tube in the larger, *super-tube*.[9,19] In a star/linear polymer blend, the entangled volume fraction of unrelaxed arms before and after disappearance of linear chains is $\Phi(\tau_d) = 1 - (\phi_s + \phi_l\sqrt{2n_a/n_l})s_d$ and $\Phi(s_d) = \phi_s(1 - s_d)$, respectively.[1] The number of entanglements in the original tube spanned by a single supertube entanglement is therefore $N_e[\Phi(s_d)]/N_e[\Phi(\tau_d)] = (\Phi(\tau_d)/\Phi(s_d))^\alpha$. The constraint release relaxation time τ_C for a single arm entanglement can therefore be estimated using the classical formula[7-9]

$$\tau_C = \tau_d\left(\frac{N_e[\Phi(s_d)]}{N_e[\Phi(\tau_d)]}\right)^2 = \tau_d\left[\frac{\Phi(\tau_d)}{\Phi(s_d)}\right]^{2\alpha}$$

If the length of unrelaxed arm $N_a' = N_a(1 - s_d)$ at $t = \tau_d$ is less than the supertube entanglement spacing $N_e[\Phi(s_d)]$, all arm constraints would have already disappeared at a time

$$\tau_C' = \tau_d\left(\frac{N_e[\Phi_{eq}]}{N_e[\Phi(\tau_d)]}\right)^2 = \tau_d\left(\frac{N_a'}{N_e}\Phi(\tau_d)^\alpha\right)^2 \qquad (1)$$

i.e. earlier than τ_C. The stress held by the remaining

arm will therefore relax sooner than anticipated from τ_C. Here $(N_a'/N_e(\Phi_{eq})) = 1$ at the point of disentanglement and $N_e(\Phi_{eq}) = N_e\Phi_{eq}^{-\alpha}$. The entangled volume fraction at $t = \tau_C'$ can now be determined from equation (A11),

$$\Phi_{eq} = \Phi(\tau_d)\left[\frac{\tau_d}{\tau_C'}\right]^{1/2\alpha} \tag{2}$$

Since $\tau_C' < \tau_C$ the original tube is only allowed to explore a region of diameter $a_{eq} \sim \Phi_{eq}^{-\alpha/2}$ in the larger super tube diameter $a(s_d) \sim \Phi(s_d)^{-\alpha/2}$ before the initial stress is forgotten.

The complex modulus $G(\omega)$ for a dilute star/linear polymer blend at low frequencies can now be written as

$$\frac{G(\omega)}{G_N} = (1+\alpha)\phi_s \int_0^{s_d}(1 - VF_s s_s)^{\alpha}\frac{i\omega\tau_{s,b}(s_s)}{1 + i\omega\tau_{s,b}(s_s)}\,ds_s \quad \text{(star arm in DD)}$$

$$+ (1+\alpha)\phi_l\int_0^{s_L}(1 - VF_l s_l)^{\alpha}\frac{i\omega\tau_{l,b}(s_l)}{1 + i\omega\tau_{l,b}(s_l)}\,ds_l \quad \text{(linear-half arm in DD)}$$

$$+ \Phi(\tau_d)^{\alpha}[\Phi(\tau_d) - \phi_s(1 - s_d)]\frac{i\omega\tau_d}{1 + i\omega\tau_d} \quad \text{(reptation of linear chain)}$$

$$+ \phi_s(1 - s_d)\psi\int_{\tau_d}^{\tau_C'}\frac{\Phi(\tau)^{\alpha}}{2\tau}\frac{i\omega\tau}{1 + i\omega\tau}\,d\tau \quad \text{(Rouse motion in CR)} \tag{3}$$

where the volume fraction VF_i is defined in the appendix and $\psi = (a_{eq}^2 L_a/a(s_d)^2 L_a) = [(\Phi(s_d)/\Phi_{eq})]^{\alpha}$ is the ratio of the volumes of the *supertube* and *exploration* tube, respectively. Notice that if $N_a' \geq N_e[\Phi(s_d)]$, $\tau_C' = \tau_C$, $\Phi_{eq} = \Phi(s_d)$, and the original CR result is recovered as expected. Furthermore, if $N_a' > N_e[\Phi(s_d)]$, relaxation continues after CR by arm retraction. Thus, the criterion for RDD can finally be written: $(N_a(1 - s_d)\Phi(s_d)^{\alpha}/N_e) > 1$.

Figures 8−10 compare experimental $G'(\omega)$ and $G''(\omega)$ data for 2%, 5%, and 10% star/linear polymer blends with results predicted using eq 3. The same model parameters as before are used for the comparisons, and α is fixed to a value of $^4/_3$. Overall, the predictions, particular for $G''(\omega)$, are clearly closer to the experimental results with a few exceptions. Experimental results for blends containing the two lowest molecular weight linear polymers (SL18K and SL48K) are substantially lower than the predictions over the entire frequency range. However, closer scrutiny of the data indicate that horizontal translation of the theoretical curves by factors of 2 and 3, respectively, significantly reduces the discrepancy between theory and experiments, suggesting that the actual value of τ_e in these blends may be somewhat lower than the value $\tau_e = 2.4 \times 10^{-7}$ s used for the calculations.

Figures 11 and 12 compare the M_L dependence of the zero-shear viscosity $\eta_0 = \lim_{\omega\to 0}(G''(\omega)/\omega)$ and terminal relaxation time $\tau_{d0} \equiv \eta_0 J_e^0$ of two dilute star/linear blends obtained using eq 3 and from experiment. For

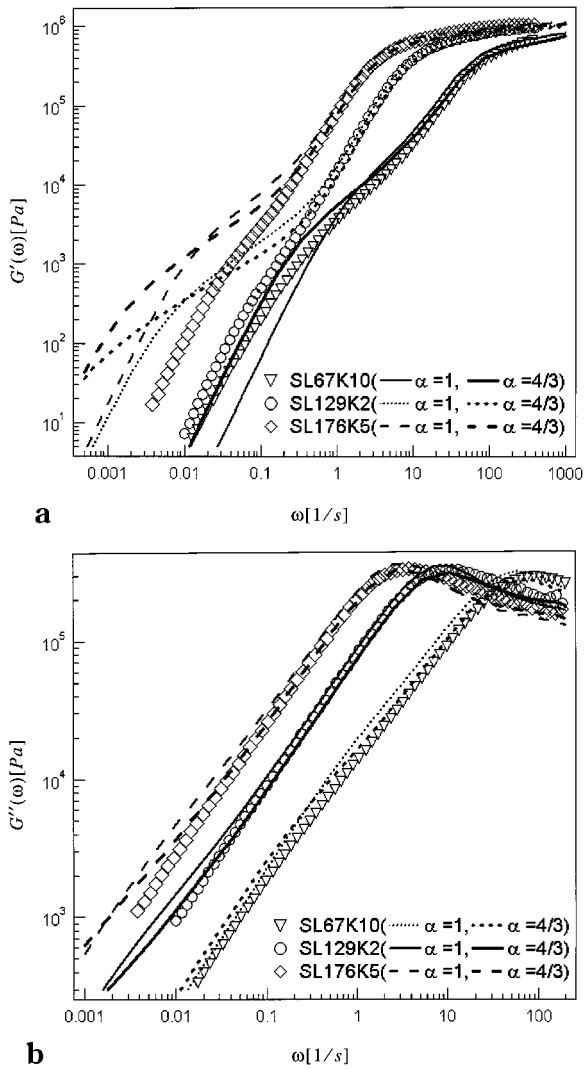

Figure 7. Experimental storage and loss moduli, (a) $G'(\omega)$ and (b) $G''(\omega)$, for SL67K10, SL129K2, and SL176K5 compared with MM model predictions without recovery of dynamic dilution, $\alpha = 1$ (thin line) and $\alpha = {}^4/_3$ (thick line).

both materials, the experimental and theoretical zero-shear viscosities (Figure 11) compare very well over the entire range of M_L. Best-fit line through the theoretical η_0 results for the 2%, 5%(not shown), and 10% series blends support a relationship between η_0 and M_L of the form $\eta_0 \sim M_L^{2.9\pm0.1}$. Theoretical and experimental terminal times (Figure 12) do not compare as well. Unlike $G'(\omega)$ comparisons, the largest disagreements are not restricted to low M_L values. Nevertheless, considering that fact that the model contains no adjustable parameters, the agreement is still considered fair. In this case, a scaling relationship of the form good to excellent accord over the range of M_L values studied. The effect of M_L on τ_{d0} is consistent with other experimental results[3,4] and with the constraint release relaxation time predicted by Brochard-Wyart et al.[10] using a very different approach. This last finding is perhaps surprising since the conventional expression for the constraint release relaxation time[7] is used in the analysis. We believe that the improved terminal properties arise from more accurate description of the tube-diameter evolution in the final regime of relaxation. Taken together with the $G'(\omega)$ and $G''(\omega)$ comparisons, these results indicate that relaxation dynamics in star/linear polymer blends with low ϕ_s are fairly described by the MM model with

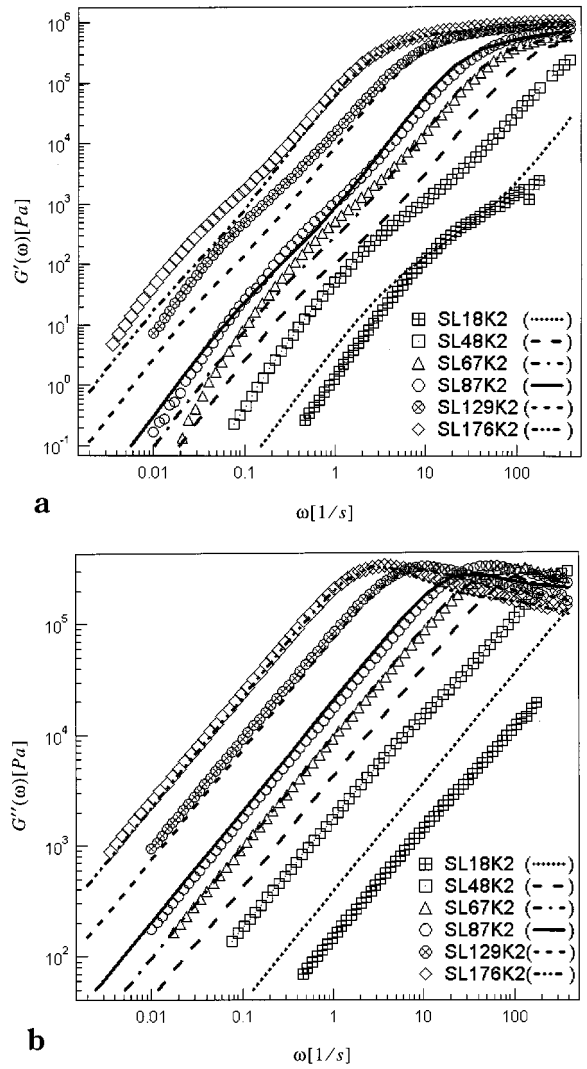

Figure 8. Storage and loss moduli ((a) $G'(\omega)$ and (b) $G''(\omega)$) data for SL18K2, SL48K2, SL67K2, SL87K2, SL129K2, and SL176K2. The solid lines through the data are obtained using eq 3. The same model parameters used to compare MM model predictions with experimental results are employed throughout.

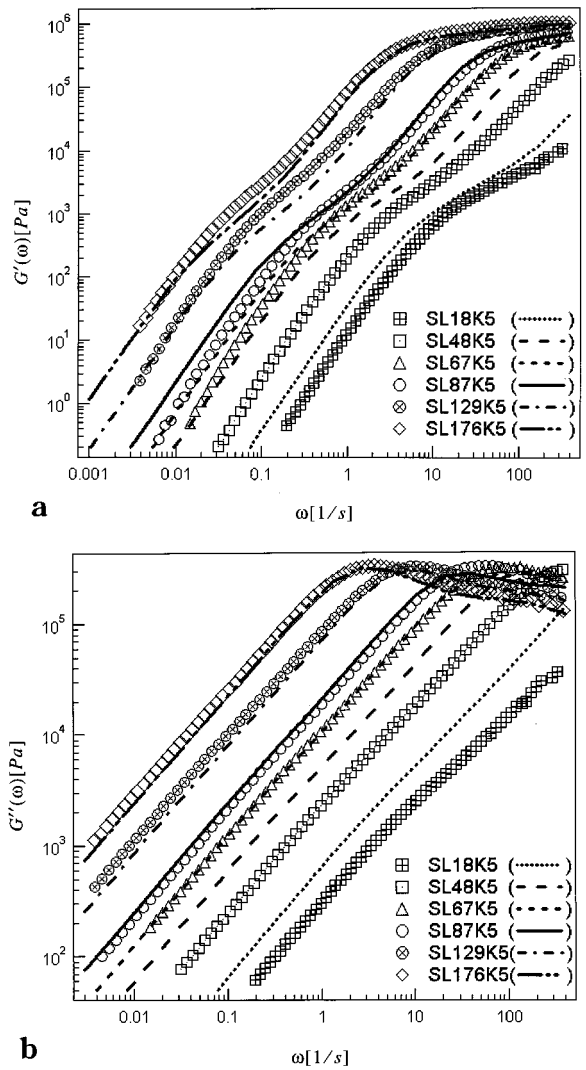

Figure 9. Storage and loss moduli ((a) $G'(\omega)$ and (b) $G''(\omega)$) data for SL18K5, SL48K5, SL67K5, SL87K5, SL129K5, and SL176K5. Solid lines through the data are predictions from eq 3.

the suggested modification. The situation in star/linear blends with higher star polymer concentrations is, however, much more complicated. Specifically, even with the proposed changes, the MM model appears to disagree with the very limited experimental data available. We therefore postpone detailed discussion of these systems for a future article.

Conclusions

Stress relaxation dynamics in a series of star/linear 1,4-polybutadiene blends were investigated experimentally using oscillatory shear flow measurements. Experimental storage and loss moduli, $G'(\omega)$ and $G''(\omega)$, were compared with predictions of a theory for star-linear polymer blend dynamics proposed by Milner and McLeish. For star/linear blends with moderate star polymer concentrations ϕ_s, the theoretical $G'(\omega)$ and $G''(\omega)$ predictions are found to be in excellent accord with experimental results. The quality of the theoretical predictions decrease however as star polymer concentration is varied in either direction (i.e., higher and lower). Theoretical predictions are, for example, found to be considerably worse at $\phi_s \leq 0.1$ and $\phi_s \geq 0.5$ than at $\phi_s = 0.28$. The greatest discrepancies between theory and experimental results for the low ϕ_s blends are observed at oscillation frequencies $\omega \leq \omega_d$, where $\omega_d^{-1} \sim M_L^{3.4\pm0.25}$ is approximately the terminal time of linear polymer molecules in the blends.

An amended version of the MM model is developed to better describe the final stages of relaxation of star arms in star/linear polymer blends. The model is based on the idea that, after linear chains relax, star arms initially relax as if they are confined in the same tube as before linear polymer relaxation. The arms explore the larger *supertube* in a series of impulsive Rouse-like hops that can either end with complete relaxation if the explored tube diameter becomes comparable to the coil size of the unrelaxed arm segments, or can end by loss of a single entanglement constraint when the explored diameter becomes comparable to the supertube diameter. A new criterion, $(N_a(1 - s_d)\Phi(s_d)^\alpha/N_e) < 1$, is proposed on this basis for determining whether relaxation goes to completion or whether arm retraction dynamics are recovered after relaxation of the linear chains. Storage and loss moduli predicted using the new approach generally compare more favorably with ex-

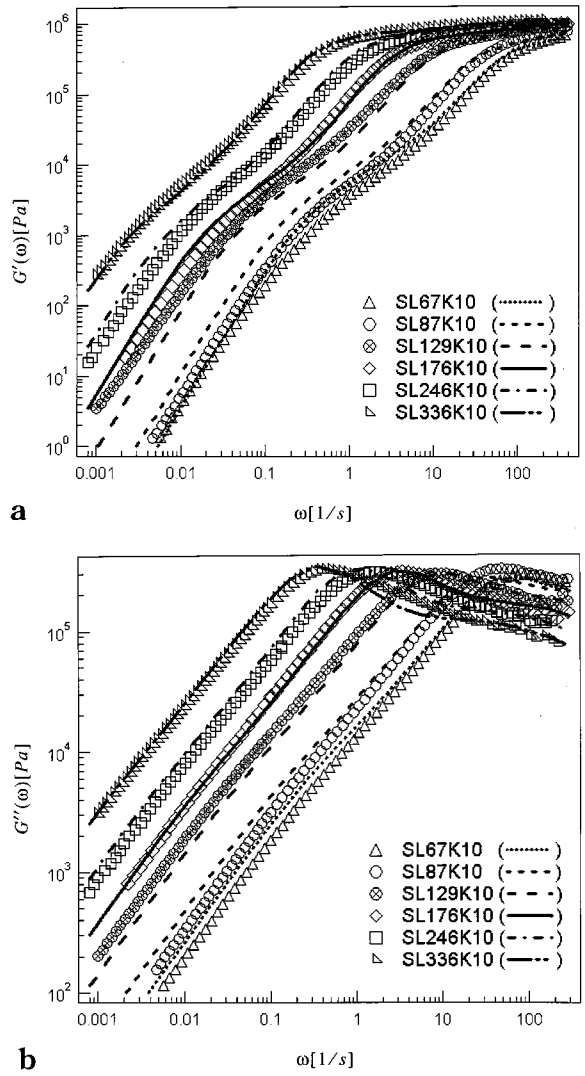

Figure 10. Storage and loss moduli ((a) $G'(\omega)$ and (b) $G''(\omega)$) data for SL67K10, SL87K10, SL129K10, SL176K10, SL246K10, and SL336K10. Solid lines through the data are predictions from eq 3.

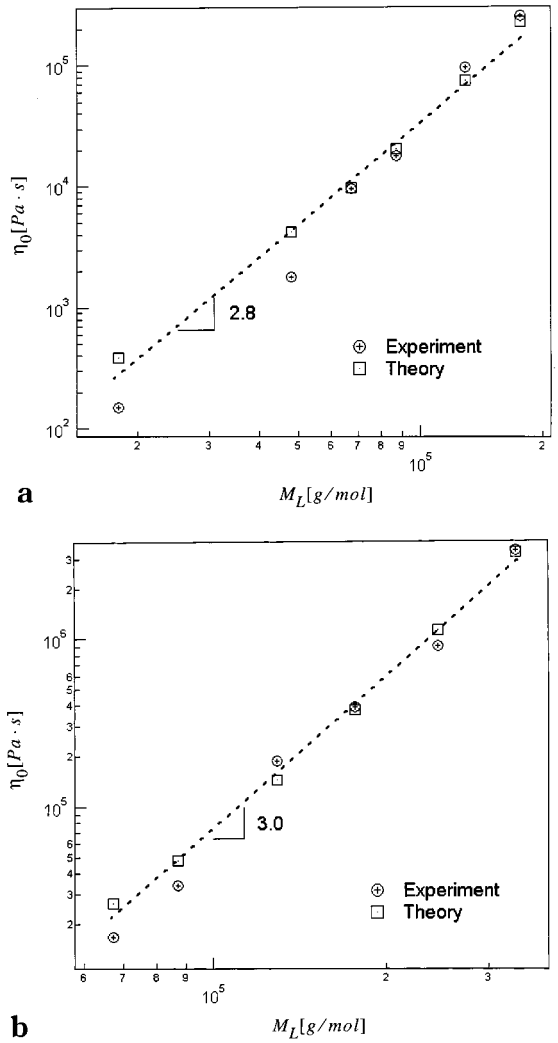

Figure 11. Limiting shear viscosity η_0 for star linear blends ((a) with $\phi_s = 0.02$; (b) with $\phi_s = 0.1$) from experiment (circles) and from eq 3 (rectangles). The straight lines through the data indicate the dependence of theoretical η_0 values on the molecular weight of linear molecules, M_L.

perimental results at low ϕ_s. Terminal properties computed from the analysis are also found to be in much better accord with experiments.

These changes to the MM model do not improve theoretical predictions in star/linear blends with high ϕ_s. In this case, the magnitude of discrepancies between predicted and experimental results suggest that additional modes of relaxation in star/linear blend systems must be considered in tube model theories. For example, a recent analysis of molecular friction in star/linear polymer blends indicates that a new activated constraint release regime should exist in these materials.[6] This CR regime is, however, not captured by the MM model. In addition, Watanabe et al.[21−23] recently reported failure of dynamic dilution in monodisperse star polymers due to slower than expected CR equilibration. We suspect that both mechanisms may be needed to correctly describe relaxation dynamics of star/linear blends with high star polymer volume fractions.

Acknowledgment. The authors are grateful to the National Science Foundation (Grant No. DMR9816105) for supporting this study.

Appendix

The MM star/linear blend model[1] was modified to accommodate arbitrary values of α as follows.

In the dynamic dilution (DD) regime ($0 < s_s < s_d$ and $0 < s_l < s_d\sqrt{(2n_a/n_l)}$. $n_i = (N_i/N_e)$ and ϕ_i is the volume fraction of star s or linear l polymer. Equation 3 in ref 1 is modified as follows:

$$\Phi(s_s) = 1 - VF_s s_s = 1 - \left(\phi_s + \phi_l\sqrt{\frac{2n_a}{n_l}}\right)s_s \quad \text{(A1)}$$

$$\Phi(s_l) = 1 - VF_l s_l = 1 - \left(\phi_l + \phi_s\sqrt{\frac{n_l}{2n_a}}\right)s_l \quad \text{(A2)}$$

$$U_{s,b}(s_s) = \frac{15}{4}n_a\frac{1-(1-VF_s s_s)^{\alpha+1}[1+(1+\alpha)VF_s s_s]}{VF_s{}^2(1+\alpha)(2+\alpha)} \quad \text{(A3)}$$

$$U_{l,b}(s_l) = \frac{15}{4}\frac{n_l}{2}\frac{1-(1-VF_l s_l)^{\alpha+1}[1+(1+\alpha)VF_l s_l]}{VF_l{}^2(1+\alpha)(2+\alpha)} \quad \text{(A4)}$$

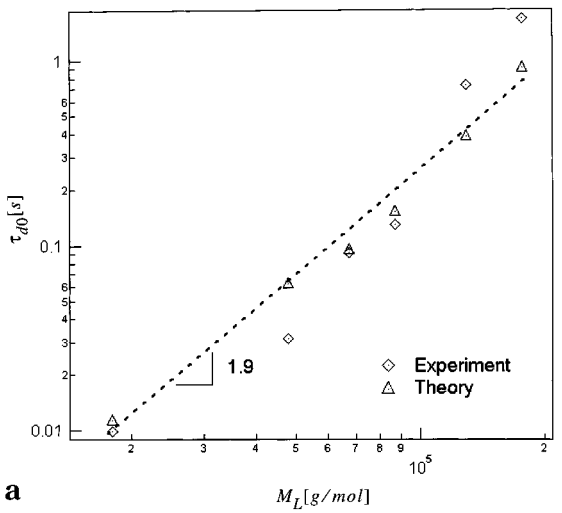

a

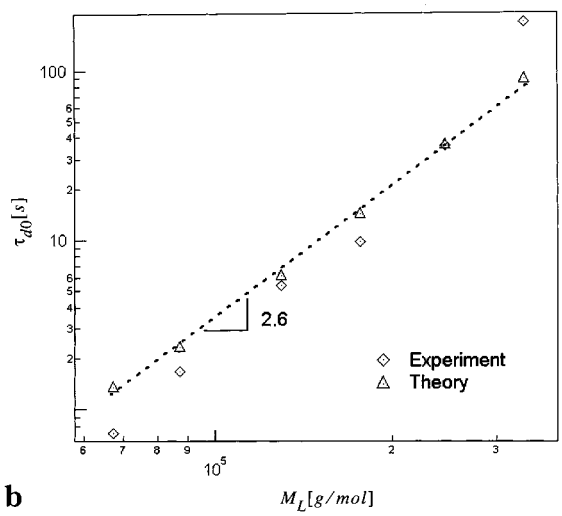

b

Figure 12. Terminal relaxation time τ_{d0} for star linear blends ((a) with $\phi_s = 0.02$; (b) with $\phi_s = 0.1$) from experiment (diamonds) and from eq 3 (triangles). The straight lines through the data indicate the dependence of τ_{d0} values from theory on the molecular weight of linear molecules, M_L.

The *early fast diffusion* time of star and linear polymers is given by eq 13 in ref 20.

$$\tau_{early}(s_s) = \frac{225\pi^3}{256}\tau_e n_a{}^4 s_s{}^4 \quad \text{(A5)}$$

$$\tau_{early}(s_s) = \frac{225\pi^3}{256}\tau_e \left(\frac{n_l}{2}\right)^4 s_l{}^4 \quad \text{(A6)}$$

For s values far away unity, $\tau_{late}(s) \approx (L^2/D_{eff})(\sqrt{\pi/2U_{eff}''(0)})(\exp[U_{eff}(s)]/U_{eff}'(s))$, while for s near unity, $\tau_{late}(s) \approx (L^2/D_{eff})(\pi \exp[U_{eff}(s)])/(\sqrt{|U_{eff}''(s)|U_{eff}''(0)})$. Except in situations where $N_L \gg N_s$, linear molecules are anticipated to reptate much faster than the arms retract, so that the first situation better describes arm dynamics prior to complete disappearance of entanglements with linear molecules

$$\tau_{late}(s_s) = \tau_e n_a{}^{3/2} \sqrt{\frac{\pi^5}{30}} \frac{\exp[U_{s,b}(s_s)]}{s_s(1 - VF_s s_s)^\alpha} \quad \text{(A7)}$$

$$\tau_{late}(s_l) = \tau_e \left(\frac{n_l}{2}\right)^{3/2} \sqrt{\frac{\pi^5}{30}} \frac{\exp[U_{l,b}(s_l)]}{s_l(1 - VF_l s_l)^\alpha} \quad \text{(A8)}$$

The final arm retraction time $\tau_{i,b}(s_i)$ for $i = \{s,l\}$in the DD regime is

$$\tau_{i,b}(s_i) = \frac{\tau_{early}(s_i)}{1 + \exp[U_{i,b}(s_i)]\tau_{early}(s_i)/\tau_{late}(s_i)} \times \exp[U_{i,b}(s_i)] = P_{i,b}(s_i)\exp[U_{i,b}(s_i)] \quad \text{(A9)}$$

The repatation time of the linear chains, τ_d, and the fractional position of the first unrelaxed arm segment, s_d, at $t = \tau_d$ are obtained by solving $\tau_d = (15/4)n_l{}^3(1 - s_d\sqrt{2n_a/n_l})^2\tau_e = \tau_{s,b}(s_d)$.

In the constraint-release (CR) regime ($s_s = s_d$)

$$\Phi(t)^\alpha = \Phi(\tau_d)^\alpha \sqrt{\frac{\tau_d}{t}} \quad \text{(A10)}$$

As a result, eq 15 in ref 1 becomes

$$\tau_C = \tau_d \left(\frac{\Phi(\tau_d)}{\Phi(s_d)}\right)^{2\alpha} \quad \text{(A11)}$$

The time-dependent modulus $G(t) = G_N\phi_s(1 - s_d)\Phi(t)^\alpha$ in the time interval between τ_d and τ_C can now be rewritten as

$$G(t) = -\int_{\tau_d}^{\tau_C} \frac{\partial G}{\partial \Phi}\frac{\partial \Phi}{\partial \tau}\exp\left[-\frac{t}{\tau}\right] d\tau = G_N\phi_s(1 - s_d)\int_{\tau_d}^{\tau_C} \frac{\Phi(\tau)^\alpha}{2\tau}\exp\left[-\frac{t}{\tau}\right] d\tau \quad \text{(A12)}$$

Finally in the recovery of dynamic dilution regime (RDD), ($s_d < s_f < 1$),

$$\tau_{late}(s_f) = \tau_e \left(\frac{n_a}{\phi_s{}^\alpha}\right)^{3/2} \times \sqrt{\frac{\pi^5}{30}} \frac{\exp[U_{RDD}(s_f)]}{s_f\sqrt{(1 - s_f)^{2\alpha} + \left[\frac{4(\alpha+1)}{15 n_a \phi_s{}^\alpha}\right]^{2\alpha/\alpha+1}\left[\Gamma\left(\frac{1}{\alpha+1}\right)\right]^{-2}}} \quad \text{(A13)}$$

where

$$U_{RDD}(s_f) = \phi_s{}^\alpha U_{eff}(s_f);$$

$$U_{eff}(s) = \frac{15}{4}\frac{N_a}{N_e}\frac{1 - (1 - s)^{\alpha+1}[1 + (1 + \alpha)s]}{(1 + \alpha)(2 + \alpha)}$$

The relaxation time $\tau_{RDD}(s_f)$ is the same as given by eq 20 of ref 1

$$\tau_{RDD}(s_f) = \tau_C \frac{P_{RDD}(s_f)}{P_{RDD}(s_d)}\exp[U_{RDD}(s_f) - U_{RDD}(s_d)] \quad \text{(A14)}$$

where $P_{RDD}(s_f)$ is same to $P_{i,b}(s_i)$ in eq A9.

The full expression for $G(\omega)$ is

$$G(\omega) = G_N(1+\alpha)\phi_s\int_0^{s_d}(1-VF_s s_s)^\alpha \frac{i\omega\tau_{s,b}(s_s)}{1+i\omega\tau_{s,b}(s_s)}\,ds_s \quad \text{(star arm in DD)}$$

$$+ G_N(1+\alpha)\phi_l\int_0^{s_L}(1-VF_l s_l)^\alpha \frac{i\omega\tau_{l,b}(s_l)}{1+i\omega\tau_{l,b}(s_l)}\,ds_l \quad \text{(linear-half arm in DD)}$$

$$+ G_N\Phi(\tau_d)^\alpha[\Phi(\tau_d)-\phi_s(1-s_d)]\frac{i\omega\tau_d}{1+i\omega\tau_d} \quad \text{(reptation of linear chain)}$$

$$+ G_N\phi_s(1-s_d)\int_{\tau_d}^{\tau_C}\frac{\Phi(\tau)^\alpha}{2\tau}\frac{i\omega\tau}{1+i\omega\tau}\,d\tau \quad \text{(Rouse motion in CR)}$$

$$+ G_N(1+\alpha)\phi_s^{\alpha+1}\int_{s_d}^1(1-s_f)^\alpha\frac{i\omega\tau_{RDD}(s_f)}{1+i\omega\tau_{RDD}(sf)}ds_f \quad \text{(remaining arm segments in RDD)} \quad \text{(A15)}$$

References and Notes

(1) Milner, S. T.; McLeish, T. C. B.; Young, R. N.; Hakiki, A.; Johnson, J. M. *Macromolecules* **1998**, *31*, 9345.
(2) Larson, R.G. *Macromolecules* **2001**, *34*, 4556.
(3) Roovers, J. *Macromolecules* **1987**, *20*, 148.
(4) Watanabe, H.; Yoshida, H.; Kotaka, T. *Macromolecules* **1988**, *21*, 2175.
(5) Struglinski, M. J.: Graessley, W. W.; Fetters, L. J. *Macromolecules* **1988**, *21*, 783.
(6) Lee, J. H.; Archer, L. A. *J. Polym. Sci., Part B: Polym. Phys.* **2001**, *39*, 2501.
(7) Daoud, M.; de Gennes, P. G. *J. Polym. Sci., Part B: Polym. Phys.* **1979**, *17*, 1971.
(8) Doi, M.; Graessley, W. W.; Helfand, E.; Pearson, D. S. *Macromolecules* **1987**, *20*, 1900.
(9) Viovy, J. L.; Rubinstein, M.; Colby, R. H. *Macromolecules* **1991**, *24*, 3587.
(10) Brochard-Wyart, F,; Ajdari, A.; Leibler, L.; Rubinstein, M.; Viovy, J. L. *Macromolecules* **1994**, *27*, 803.
(11) Mhetar, V. R.; Archer, L. A. *Macromolecules* **1998**, *31*, 6639.
(12) Ball, R. C.; McLeish, T. C. B. *Macromolecules* **1989**, *22*, 1911.
(13) Pearson, D. S.; Helfand, E. *Macromolecules* **1984**, *17*, 888.
(14) Bueche, F. *J. Chem. Phys.* **1952**, *20*, 1959.
(15) Doi, M.; Edwards, S. F. *The Theory of Polymer Dynamics*; Oxford University Press: New York, 1986.
(16) Juliani; Archer, L. A. *J. Rheol.* **2001**, *45*, 691.
(17) Islam, M. T.; Juliani; Archer, L. A.; Varshney, S. K. *Macromolecules* **2001**, *34*, 6438.
(18) Colby, R. H.; Rubinstein, M. *Macromolecules* **1990**, *23*, 2753.
(19) Milner, S. T. *J. Rheol.* **1996**, *40*, 303.
(20) Milner, S. T.; McLeish, T. C. B. *Macromolecules* **1997**, *30*, 2159.
(21) Watanabe, H.; Matsumiya, Y.; Osaki, K. *J. Polym. Sci., Part B: Polym. Phys.* **2000**, *38*, 1024.
(22) Matsumiya, Y.; Watanabe, H. *Macromolecules* **2001**, *34*, 5702.
(23) Watanabe, H.; Matsumiya, Y.; Inoue, T. *Macromolecules* **2002**, *35*, 2339.

MA020398E